



ORIGINAL ARTICLE

Comparative investigation of aerial part and root in *Lamiophlomis rotata* using UPLC-Q-Orbitrap-MS coupled with chemometrics



Tong Li, Li Jia, Ruijiao Du, Chengjuan Liu, Shengjie Huang, Heshui Yu, Lifeng Han, Xiaopeng Chen, Yuefei Wang, Miaomiao Jiang*

State Key Laboratory of Component-based Chinese Medicine, Tianjin University of Traditional Chinese Medicine, Tianjin 301617, China

Received 3 December 2021; accepted 24 January 2022

Available online 29 January 2022

KEYWORDS

Lamiophlomis rotata (Benth.)
Kudo;
Different parts;
Comparative investigation;
Non-targeted metabolomics;
UPLC/Q-Orbitrap MS

Abstract *Lamiophlomis rotata* (Benth.) Kudo (*L. rotata*) belongs to *Lamiaceae* family, which is an important medicinal plant endemic to Qinghai Tibet Plateau. Traditionally, the whole herb of *L. rotata* is used for medicine, especially for the treatment of rheumatoid arthritis (RA) in clinical practice. As a result of absolute digging, the plant has a long regeneration cycle after excavation and the damage to plateau grassland ecological environment is difficult to recover. It has been encouraged to use aerial part of the plant with the purpose of protecting environment and maintaining biological diversity. At present, researchers have compared the primary metabolites and iridoids between aerial parts and roots, but there are few reports on the chemical differences and activity comparison of secondary metabolites. In order to characterize the secondary metabolites of different parts, UPLC/Q-Orbitrap-MS was employed to collect data from the extracts of aerial parts and roots, in combination with plant metabolomics technology to screen and quantify differential metabolites. At the same time, network pharmacological analysis with rheumatoid arthritis and immunity as the key words was carried out according to the identification results to clarify the active ingredients of *L. rotata* in the treatment of RA, so as to speculate the pharmacological effects of aerial parts and roots based on the distribution of active components. A total of 16 potential markers were selected and identified to differentiate two parts. Among them, 8 characteristic flavonoids with similar skeletons were unique in aerial parts, while the other 8 components, including 2 iridoid glycosides and 6 phenylethanoid glycosides, were detected in both aerial parts and roots, but with differentiate contents. Among the predicted 6 active components, there were 5 flavonoids, of which 3 (namely luteolin, apigenin and 2''-acetylastragalol) were still differential metabolites and mainly distributed in

* Corresponding author.

E-mail address: miaomiaojiang@tjutcm.edu.cn (M. Jiang).

Peer review under responsibility of King Saud University.



the aerial parts. The results revealed that certain flavonoids as potential markers made a distinction between aerial part and root of *L. rotata*, and were the main active components against RA, which provided a theoretical basis for the aerial parts to replace the whole herbs, and laid a material foundation for further pharmacological research.

© 2022 The Authors. Published by Elsevier B.V. on behalf of King Saud University. This is an open access article under the CC BY-NC-ND license (<http://creativecommons.org/licenses/by-nc-nd/4.0/>).

1. Introduction

Lamiophlomis rotata (Benth.) Kudo (*L. rotata*) is a plant in *Lamiaceae* family, which is a traditional Tibetan medicine and an important medicinal plant in the Qinghai Tibet Plateau (Jiangsu New Medical College, 1977). It was first published in the “Four Medical Tantras” and “Yuewang Medicine Diagnosis”. Traditionally, it has the effects of promoting blood circulation, stopping bleeding, dispelling wind and relieving pain, and is widely used to treat traumatic injuries and rheumatoid arthritis (RA) in clinical practice (Zeng et al., 2001; Zhao, 2004; Cui et al., 2020). At present, the chemical components isolated and identified from *L. rotata* include flavonoids, iridoid glycosides and phenylethanoid glycosides (Luo et al., 2007; Ji et al., 2007; Zhang et al., 2012; Fan et al., 2016; Kang et al., 2012; Jiang et al., 2010b; Jiang et al., 2010c; Yue et al., 2013; Dong et al., 2014). Modern pharmacological studies have shown that these secondary metabolites have many aspects and levels of efficacy. The researches have found that flavonoids have anti-inflammatory and antibacterial effects (Jiang et al., 2010a; Zhang et al., 2021), and iridoid glycosides and phenylethanoid glycosides possess hemostatic and analgesic properties (Li et al., 2009; Zhang et al., 2011; Jia et al., 2005; Zheng et al., 2015).

The growth environment of *L. rotata* is special, existing all year round in alpine grasslands or gravel beaches above 3000 m (Liu et al., 2006). In the past few years, roots and whole herbs were mainly used as medicine (Pan et al., 2015b). Excessive excavation caused serious damage to the ecological environment of plateau grassland, and it was difficult to recover. In addition, this dwarf herb had a long regeneration cycle, and digging its roots would lead to low yield. (China Pharmacopoeia Committee, 2005; China Pharmacopoeia Committee, 2010). Therefore, the limited distribution and poor growth once made *L. rotata* turn into an endangered Tibetan medicine. In order to alleviate this situation, it has encouraged to use the aerial parts as a medicinal position to protect the ecological environment and maintain biodiversity. At present, some researchers have distinguished the primary metabolites in different parts by NMR (Pan et al., 2015b), and some have compared the content and antioxidant capacity of iridoid glycosides in aerial and underground parts (Zhang et al., 2018). In this research, we mainly focused on the whole secondary metabolites to study the distribution of various components in aerial part and root and preliminarily explore the active ingredients of *L. rotata* to treat RA.

From the perspective of a global view of metabolism and characterization, non-targeted metabolomics technology has unique advantages. It is an independent part of systems biology, and has been applied in many fields, such as animals, plants and microorganisms (Mendes, 2006; Lee et al., 2014; Kim et al., 2012; Ku et al., 2009; Kim et al., 2015). Due to high

sensitivity and resolution, ultra performance liquid chromatography-mass spectrometry (UPLC-MS) has become the most widely used analysis platform in metabolomics (Han et al., 2015). Network pharmacology is a commonly used component-disease target association method, which can accelerate the identification of drug targets and the discovery of biomarkers (Wang et al., 2019). As many secondary metabolites as possible were collected by UPLC-MS, and the data were processed and analyzed by non-targeted metabolomics method, which could be used for chemical composition identification and differential metabolite screening. Through network pharmacology prediction, the distribution of each active ingredient in the aerial part and root could be cleared.

In this study, UPLC/Q-Orbitrap MS combined with non-targeted metabolomics was used to analyze the collected data and screen the potential markers. At the same time, the network pharmacological analysis of each component was performed to further clarify the basis for distinguishing the aerial part and root of *L. rotata* based on the distribution of active components in different parts, which provided a methodological reference for the comparison of the compositional differences in different parts of traditional Chinese medicine (TCM).

2. Materials and methods

2.1. Plant material

The plant was collected from Mozhugongka County, Tibet Autonomous Region (30° N, 92° E, 3835 m above sea level) with 3–4 year growth period in the traditional harvest time and dried at source area, which leaves were 4–12 cm long and 5–15 cm wide, and the roots were about 7–15 cm long and 1–2 cm thick. All samples were identified by Wu Honghua, associate researcher at Tianjin University of Traditional Chinese Medicine.

2.2. Reagents and chemicals

Acetonitrile (chromatographic purity) was purchased from Fisher company (USA), formic acid (MS grade) was purchased from ACS company (USA), and distilled water was purchased from Guangzhou Watsons food and beverage company (Guangzhou, China). Specnuezhenide (internal standard, IS) was purchased from Yuanye Biological Technology Co., Ltd. (Shanghai, China, wkq20032004). All other reagents and chemicals used were analytical grade.

2.3. Sample preparation

The 15 parts power of aerial part (A) and root (R) were accurately weighed 0.1 g. The samples ultrasonically extracted

(25 k Hz, 35°C) with 900 μ L 70% methanol (v/v) and 100 μ L IS solution (4 mg/mL Specnuezhenide) for 15 min and then centrifuged (14000 r/min) for 10 min. Subsequently, the 500 μ L supernatant was diluted with an equal amount of water, centrifuged again, and the supernatant was obtained to inject for LC-MS analysis.

2.4. Chromatographic and MS conditions

The UPLC separation was performed on Ultimate 3000 UPLC System (Thermo Fisher Scientific, San Jose, CA, USA) with a CORTECS UPLC C18 column (2.1 \times 100 mm, 1.6 μ m) maintained at 35 °C. Mobile phases were 0.1% formic acid aqueous solution (A) and acetonitrile (B), with the following gradient elution procedure: 0–14 min, 5–13% B; 14–24 min, 13–20% B; 24–27 min, 20–31% B; 27–30 min, 31–95% B. The Flow rate of elution solvent was 0.3 mL/min and injection volume of samples was 2 μ L.

The mass spectrometry analysis was completed under Q-Exactive MS coupled with Q-Orbitrap MS system (Thermo Fisher Scientific, Bremen, Germany). The ESI source was equipped under the following parameters: spray voltage, -3.0 kV/+3.5 kV; capillary temperature, 320 °C; aux gas heater temperature, 350 °C; normalized collision energy, 30/40/50 V; sheath gas (N_2), 35 arb; aux gas (N_2), 10 arb; sweep gas (N_2), 0 arb. Moreover, the scanning method of Full MS/dd-MS² (TopN) was adopted. The full scan range of MS¹ was 100–1500 m/z acquired with resolution $R = 70000$, and MS² scan range was 200–2000 m/z with the resolution $R = 17500$. Dynamic exclusion was 6.0 s and isolation window was 4.0 m/z .

2.5. Data processing and analysis

In this research, non-targeted metabolomics processing flow was employed for data analysis. Firstly, the processing software Compound Discoverer 3.2 corresponding to Q-Orbitrap mass spectrometry was used to process the mass spectra data, and generate a large data matrix including retention time and peak area. Then, the above data was normalized and imported into Simca-P 14.1 software for orthogonal partial least squares discriminant analysis (OPLS-DA) to compare the overall differences and metabolic profiles of different parts, and the differential metabolites were screened under the conditions of VIP > 1 and P -value < 0.05. Finally, the selected differential metabolites were identified according to the methods of standard comparison, database comparison and literature comparison, and relatively quantified with the known concentration of IS solution.

2.6. Network pharmacology

The chemical components of *L. rotata* were determined according to the identification results of UPLC/Q-Orbitrap MS, and the corresponding targets of each component were predicted in Swiss target prediction database and selected with a score > 0.7. *L. rotata* was mainly used to treat RA, containing anti-inflammatory and immune regulation, so “rheumatoid arthritis” and “immune regulation” were searched as keywords to obtain protein targets in TTD database, DrugBank data-

base, DisGeNET database and GeneCards database, and converted them into corresponding gene names in UniProt database. The intersection targets of the component targets and the disease-related targets were entered into the String database and predicted the interaction between the two. The common targets were imported into the DAVID database for GO analysis and KEGG analysis, where GO analysis included three modules: biological process (BP), molecular function (MF), and cell composition (CC). The top 10 items of each module were selected as a histogram, and the pathways with P -value < 0.05 were kept in a bubble chart. Regarding the visual analysis, two networks were constructed by Cytoscape: an active ingredient-target interaction network and an ingredient-target-pathway network diagram of *L. rotata*.

3. Results

3.1. Secondary metabolites profiling in aerial part and root of *L. Rotata*

According to the experimental conditions described in Section 2.4, combined with standard comparison and literature comparison methods, 48 and 40 components were identified from the aerial parts and roots respectively (Wang et al., 2018; La et al., 2015; Wu et al., 2016; Zan et al., 2018; Tao et al., 2014; Fan et al., 2012), of which there were 8 characteristic components and 40 common components, mainly including flavonoids, iridoid glycosides and phenylethanoid glycosides. The UPLC-HRMS profiles of the sample solution of aerial part and root in *L. rotata* was shown in Fig. 1, and the 48 chemical components identified by mass spectrometry were detailed in Table 1.

Flavonoids were a class of compounds with high content in *L. rotata*, mainly based on luteolin and apigenin as the basic core, connecting one molecule or two molecules of sugar to form glycoside compounds. Among them, there were 11 species in aerial parts and 3 species in roots. During the cleavage process, these components were easy to lose the connected sugar group, and produce the characteristic aglycone fragments (Van der Hooft et al., 2011; Aldini et al., 2011; Fridén and Sjöberg, 2014). Taking luteolin-7-*O*- β -D-glucopyranside as an example (Sun et al., 2015), the deprotonated precursor (m/z 447.0936) was easily produced in negative ion mode, and m/z 285.0397 by neutral elimination of Glu (162 Da) was obtained. In particular, the RDA fragments m/z 151.0013 and m/z 133.0279 were characteristic products of luteolin (see fragmentation process in Fig. 2A).

Iridoid glycosides were the characteristic components of *L. rotata*, and 17 iridoid glycosides were tentatively identified in all. Due to the diversity of substitution positions and substituent groups, its characteristic fragments were difficult to determine. Generally, a molecule of hexose was lost, followed by dehydroxylation, decarboxylation or dehydration to form respective fragment ions (Es-Safi et al., 2007; Li et al., 2008; Qi et al., 2009). Taking 8-*O*-acetyl shanzhiside methyl ester as an exhibition (La et al., 2015), its precursor ion was yielded at m/z 471.1462 for $[M + Na]^+$. Typical neutral losses (NL), involving Glu (162 Da) and CH_3COOH (60 Da), were detectable in the fragmentation pathways. Diverse productions at m/z 411.1247 ($[M + Na - CH_3COOH]^+$), m/z 249.0730

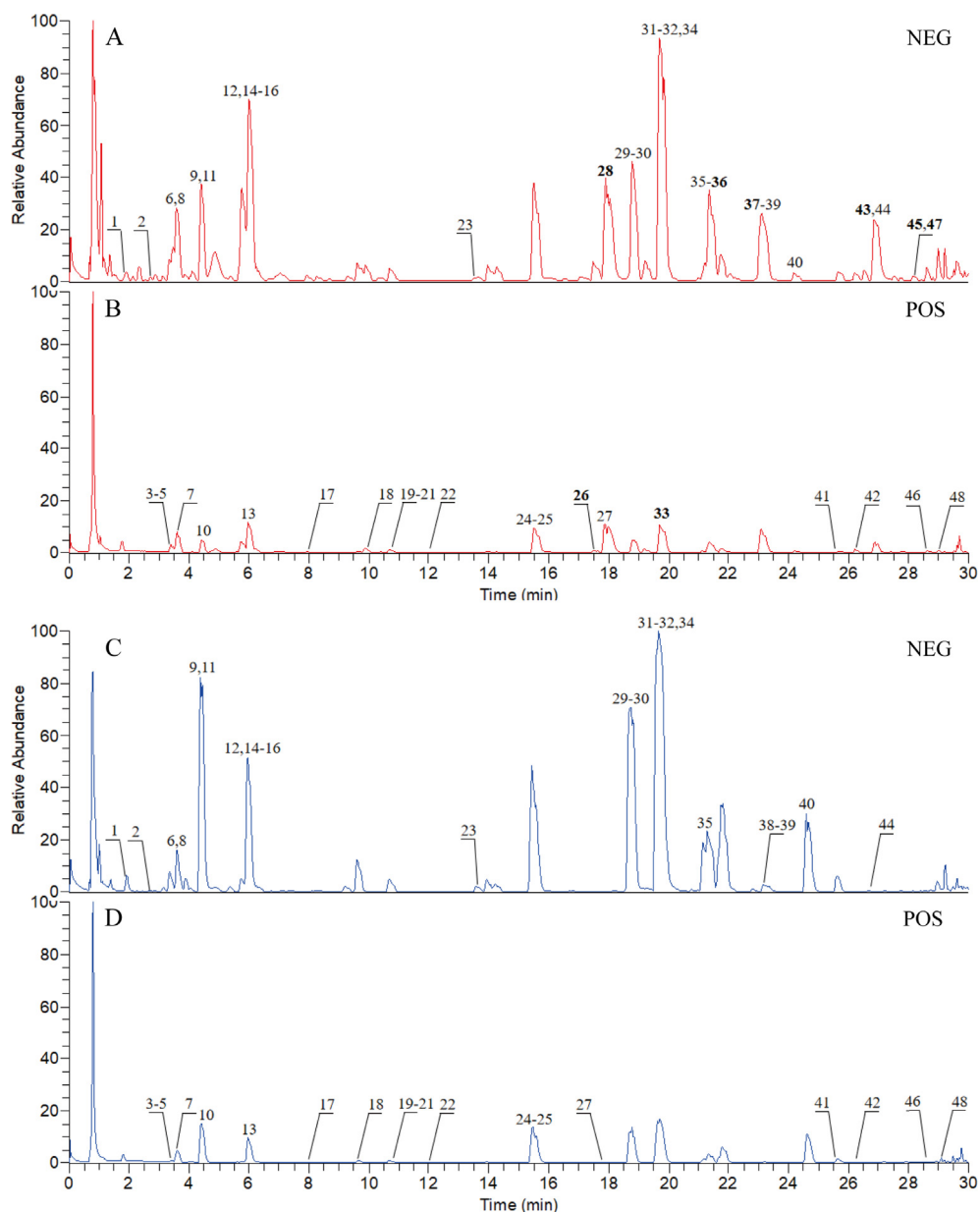


Fig. 1 The UPLC-HRMS profiles of sample solutions of aerial part and root for *Lamiophlomis rotata*, under positive and negative ionization modes. The sample in aerial part under negative ion mode (A); the sample in aerial part under positive ion mode (B); the sample in root under negative ion mode (C); the sample in root under positive ion mode (D).

($[M + Na-CH_3COOH-Glu]^+$) and m/z 231.0624 ($[M + Na-CH_3COOH-Glu-H_2O]^+$) were generated (detailed procedure in Fig. 2B).

Phenylethanoid glycosides were another significant metabolites of *L. rotata*. A total of 14 phenylethanoid glycosides were identified in aerial parts and roots. The fragmentation pathway was mainly related to breaking of ester bond or C-O bond, resulting in a series of degradation products (Sanz et al., 2012; Han et al., 2012; Amessis-Ouchemoukh et al., 2014). Taking salidroside for a witness (Guo et al., 2014), the deprotonated phenylethanol glycoside (m/z 299.1136) was readily generated. In the process of further mass spectrometry cleav-

age, an aglycone ion at m/z 137.0592 after the loss of sugar moiety (162 Da for Glu) was predominant. In another cleavage pathway, m/z 179.0698 and m/z 119.0487 were also observed (Fig. 2C).

3.2. Multivariate statistical analysis of UPLC/MS data

Non-targeted metabolomics technology has become more and more common in the study of the metabolic processes and metabolites of TCM, which can not only integrate the effective information of overall metabolites, but also compare the systematic differences between multiple groups of metabolites.

Table 1 Identification results of the chemical components of *Lamiophlomis rotata*.

Peak number	RT (min)	Compound	Formula	Calculated (Da)	Selected Ion	Precursor Ion (Da)	Error (ppm)	Attribution
1	1.91	phlomiol	C ₁₇ H ₂₆ O ₁₃	438.1373	[M + HCOO] ⁻	483.1359	0.738	A, R
2	2.62	vanillyl-β-D-glucopyranside	C ₁₄ H ₂₀ O ₈	316.1158	[M-H] ⁻	315.1089	1.140	A, R
3	3.33	lamalbid	C ₁₇ H ₂₆ O ₁₂	422.1424	[M + H] [±]	423.1487	-2.369	A, R
4	3.33	schimoside	C ₁₇ H ₂₆ O ₁₂	422.1337	[M + Na] [±]	445.1304	-5.266	A, R
5	3.36	phlorigidoside C	C ₁₇ H ₂₄ O ₁₁	404.1319	[M + H] [±]	405.1381	-2.562	A, R
6	3.76	decaffeoylverbascoside	C ₂₀ H ₃₀ O ₁₂	462.1737	[M-H] ⁻	461.1669	0.977	A, R
7	3.94	shanzhiside methyl ester	C ₁₇ H ₂₆ O ₁₁	406.1475	[M + H] [±]	407.1537	-2.672	A, R
8	4.08	salidroside	C ₁₄ H ₂₀ O ₇	300.1200	[M-H] ⁻	299.1136	-0.087	A, R
9	4.40	lamiophlomiol A/lamiophlomiol B	C ₁₁ H ₁₄ O ₆	242.2253	[M-H] ⁻	241.0699	-7.721	A, R
10	4.40	sesamoside	C ₁₇ H ₂₄ O ₁₂	420.3653	[M + Na] [±]	443.1145	-3.379	A, R
11	4.56	cistanoside F	C ₂₁ H ₂₈ O ₁₃	488.1530	[M-H] ⁻	487.1456	-0.234	A, R
12	5.74	chlorogenic acid or its isomers	C ₁₆ H ₁₈ O ₉	354.3090	[M-H] ⁻	353.0879	0.268	A, R
13	5.98	5-hydroxyloganin	C ₁₇ H ₂₆ O ₁₁	406.1461	[M + H] [±]	407.1537	-2.672	A, R
14	6.32	caffeic acid	C ₉ H ₈ O ₄	180.0423	[M-H] ⁻	179.0343	-3.809	A, R
15	6.66	chlorogenic acid or its isomers	C ₁₆ H ₁₈ O ₉	354.3090	[M-H] ⁻	353.0880	0.551	A, R
16	6.83	loganic acid	C ₁₆ H ₂₄ O ₁₀	376.3560	[M-H] ⁻	375.1299	0.613	A, R
17	7.90	phloyoside II	C ₁₇ H ₂₅ ClO ₁₂	456.1034	[M + Na] [±]	479.0914	-4.951	A, R
18	9.42	7-epi-loganin	C ₁₇ H ₂₆ O ₁₀	390.1526	[M + H] [±]	391.1590	-2.233	A, R
19	10.60	penstemoside	C ₁₇ H ₂₆ O ₁₁	406.1475	[M + Na] [±]	429.1357	-2.406	A, R
20	10.61	7,8-dehydropenstemoside	C ₁₇ H ₂₄ O ₁₁	404.1319	[M + H] [±]	405.1401	2.375	A, R
21	10.70	verbenalin	C ₁₇ H ₂₄ O ₁₀	388.3660	[M + H] [±]	389.1432	-2.630	A, R
22	11.94	loganin	C ₁₇ H ₂₆ O ₁₀	390.1526	[M + H] [±]	391.1589	-2.489	A, R
23	14.23	campnoside II	C ₂₉ H ₃₆ O ₁₆	640.2003	[M-H] ⁻	639.1936	0.848	A, R
24	14.90	rutin	C ₂₇ H ₃₀ O ₁₆	610.5175	[M + H] [±]	611.1592	-2.391	A, R
25	15.37	8-O-acetyl shanzhiside methyl ester	C ₁₈ H ₂₈ O ₁₂	448.1581	[M + Na] [±]	471.1462	-2.329	A, R
26	17.50	luteolin-7-O-β-D-apiofuranosyl (1 → 6)-β-D-glucopyranoside	C ₂₆ H ₂₈ O ₁₅	580.1428	[M + H] [±]	581.1488	-3.946	A
27	17.82	kaempferol-3-O-D-glucopyranoside	C ₂₁ H ₂₀ O ₁₁	448.3770	[M + H] ⁺	449.1065	-2.979	A, R
28	17.84	luteolin-7-O-β-D-glucopyranoside	C ₂₁ H ₂₀ O ₁₁	448.1006	[M-H] ⁻	447.0933	0.035	A
29	18.53	betonyoside A/betonyoside B	C ₃₀ H ₃₈ O ₁₆	654.2160	[M-H] ⁻	653.2094	1.059	A, R
30	18.75	forsythoside B	C ₃₄ H ₄₄ O ₁₉	756.2477	[M-H] ⁻	755.2408	0.527	A, R
31	19.69	verbascoside/isoverbascoside	C ₂₉ H ₃₆ O ₁₅	624.2054	[M-H] ⁻	623.1985	0.572	A, R
32	21.05	verbascoside/isoverbascoside	C ₂₉ H ₃₆ O ₁₅	624.2054	[M-H] ⁻	623.1983	0.251	A, R
33	21.11	apigenin-7-O-β-D-glucopyranoside	C ₂₁ H ₂₀ O ₁₀	432.1056	[M + H] [±]	433.1121	-1.901	A
34	21.37	orobanchoside	C ₂₉ H ₃₄ O ₁₅	622.1898	[M-H] ⁻	621.1831	0.977	A, R
35	21.73	alysosonide	C ₃₅ H ₄₆ O ₁₉	770.7280	[M-H] ⁻	769.2567	0.842	A, R
36	21.77	luteolin-7-O-β-D-(6''-O-acetate)-glucopyranoside	C ₂₃ H ₂₂ O ₁₂	490.1111	[M-H] ⁻	489.1038	-0.101	A
37	23.07	2''-acetylastragalol	C ₂₃ H ₂₂ O ₁₂	490.1111	[M-H] ⁻	489.1039	0.104	A
38	23.16	leucosceptoside A	C ₃₀ H ₃₈ O ₁₅	638.2211	[M-H] ⁻	637.2144	0.952	A, R
39	23.32	cistanoside C	C ₃₀ H ₃₈ O ₁₅	638.6140	[M-H] ⁻	637.2145	1.109	A, R
40	24.63	lamiophlomiside A	C ₃₆ H ₄₈ O ₁₉	784.2790	[M-H] ⁻	783.2723	0.763	A, R
41	25.72	8-epi-7-deoxyloganin	C ₁₉ H ₂₆ O ₉	374.1577	[M + Na] [±]	397.1461	-0.268	A, R
42	26.46	6β-n-butoxy-7,8-dehydropenstemoside	C ₂₁ H ₃₂ O ₁₀	444.1995	[M + H] [±]	445.2059	-2.075	A, R
43	26.88	luteolin	C ₁₅ H ₁₀ O ₆	286.0477	[M-H] ⁻	285.0407	0.838	A
44	27.01	martynoside	C ₃₁ H ₄₀ O ₁₅	652.6400	[M-H] ⁻	651.2302	1.162	A, R
45	28.58	apigenin-7-O-(6''-O-4-coumaroyl)-β-glucopyranoside	C ₃₀ H ₂₆ O ₁₂	578.1389	[M-H] ⁻	577.1359	1.301	A
46	28.66	hyperoside	C ₂₁ H ₂₀ O ₁₂	464.3763	[M + H] [±]	465.1016	-2.478	A, R
47	28.66	apigenin	C ₁₅ H ₁₀ O ₅	270.0528	[M-H] ⁻	269.0460	1.685	A
48	29.24	salviifoside A	C ₂₀ H ₂₂ O ₉	406.1264	[M + Na] [±]	429.1162	1.390	A, R

According to the research method of metabolomics, the mass spectrum data of 30 batches of aerial parts and roots was pre-processed and predicted in Compound Discoverer 3.2 software, and then the normalized data was imported into Simca-P 14.1 software for multivariate statistical analysis.

OPLS-DA analysis is a supervised pattern recognition method, which can maximize the differences between different

groups. As reflected in Fig. 3, the aerial part and root of *L. rotata* were respectively distributed in different quadrants and had good clustering effect, indicating that there were obvious differences between different parts. In order to prevent the model from overfitting, the permutation test (200 response ranking test) was used to evaluate the model. The R²X value was 0.549 and the R²Y value was 0.989, which could be deter-

mined that the analyzed data has good adaptability to establish the model. At the same time, the Q^2 of 0.976 was able to confirm that the analytical model has good predictability.

Both VIP-value and P -value can represent the importance of variables to grouped data, and reveal potential markers. Normally, the larger the VIP-value, the more obvious the compounds in multiple batches are. On the contrary, the smaller the P -value, the more important the compound can be reflected. Currently, the data with $VIP > 1$ or P -value < 0.05 can be regarded as differential components. In this experiment, a total of 578 variables were selected under the condition of $VIP > 1$, and a total of 3737 variables were selected under the condition of P -value < 0.05 . Taking the intersection of the two, 474 important variables were screened, which would be used as potential markers for further analysis.

3.3. Identification and relative quantification of the differential metabolites

Differential metabolites can be divided into characteristic components and differential components. The characteristic components are the components that can be distinguished from other parts, and the differential components refer to the components with different contents between different parts. Using a variety of mass comparison methods to identify the differential metabolites screened above, a total of 16 components were identified. Among them, it included 8 characteristic components (Fig. 4A), mainly concentrated in aerial parts. Flavonoids occupied an absolute position, and the specific compounds were apigenin, apigenin-7- O - β -glucopyranoside, apigenin-7- O -(6''- O -4-coumaroyl)- β -glucopyranoside, luteolin,

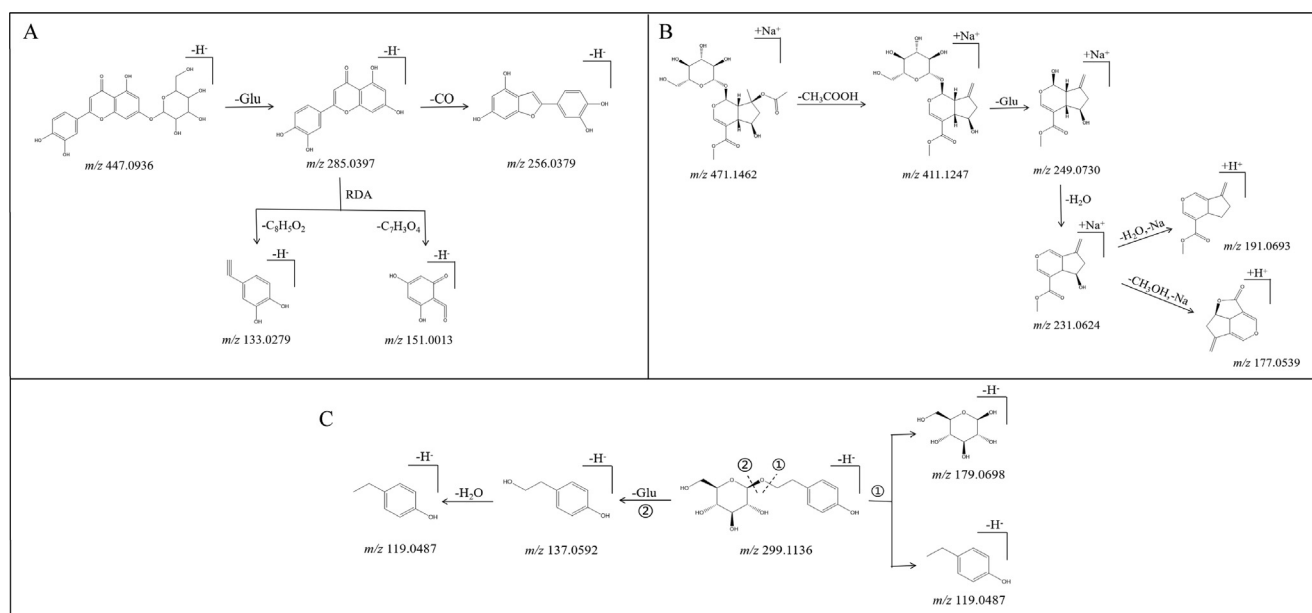


Fig. 2 Possible mass fragmentation pathways of luteolin-7- O - β -D-glucopyranoside (A), 8- O -acetyl shanzhisi methyl ester (B), and salidroside (C).

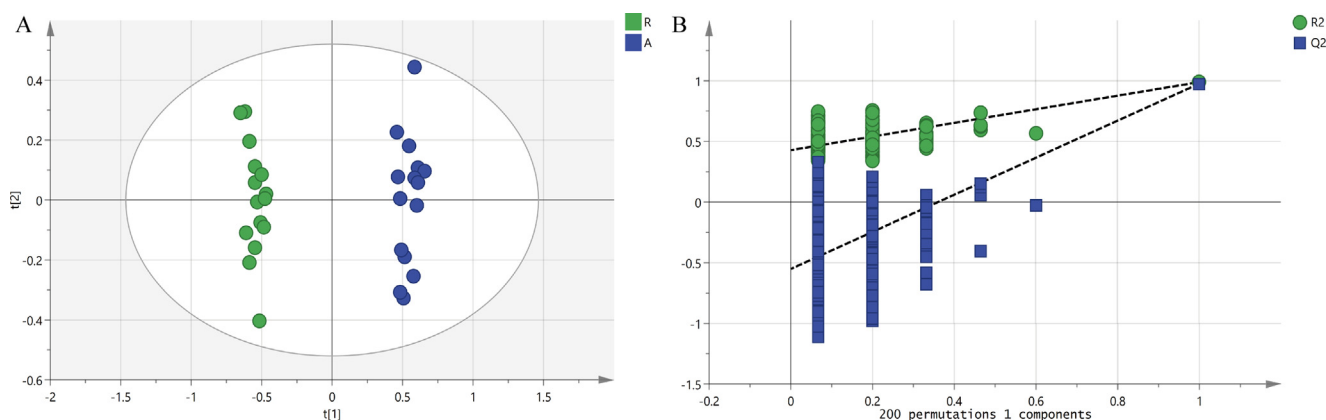


Fig. 3 Orthogonal partial least squares regression analysis (OPLS-DA) score chart (A) and 200 response ranking tests (B).

luteolin-7-*O*- β -glucopyranoside, luteolin-7-*O*- β -apiofuranosyl-(1 \rightarrow 6)- β -glucopyranoside, luteolin-7-*O*- β -(6''-*O*-acetate)-glucopyranoside, and 2''-acetylstragalin. In addition, there were also 8 different components detected in both aerial parts and roots, including 2 iridoid glycosides and 6 phenylethanoid glycosides. Phlorigidoside C, phloyoside II, salidroside, campneoside II and cistanoside F were high in aerial parts (Fig. 4B), whereas lamiophlomiside A, decaffeoylverbascoside and leucosceptoside A were high in roots (Fig. 4C).

In order to further analyze the content changes of differential metabolites in aerial parts and roots, the known concentration of IS solution was added to the samples for relative quantification. Specnuezhenide is the iridoid compound with similar chemical properties to the samples, but it is chained while the iridoid glycosides in *L. rotata* are circular. Therefore, specnuezhenide could be well dissolved in the samples without overlapping with other signal peaks during the separation process, so it was selected as the IS material. In this study, the concentration of the above differential metabolites were calculated according to the known IS solution concentration and the normalized peak area, then the content of them were derived based on the solution volume and powder mass of each batch of samples, and finally the box diagrams were made for the content information of these 16 differential metabolites. As seen in Fig. 5, the content and distribution of each component could be more intuitively distinguish (detailed in table S1).

3.4. Network pharmacology results

According to the prediction results of the above database, a total of 58 component targets, 1350 inflammation-related targets and 1992 immune-related targets were selected. There were 28 common targets in the intersection of component targets and inflammatory targets, and 28 common targets in the

intersection with immune targets. Cytoscape was introduced to construct the active ingredient-predicted target interaction network (Fig. 6A). It was obvious that luteolin, apigenin and caffeic acid had more predicted targets. In addition, the predicted active components were mainly flavonoids, indicating that flavonoids might be the main active components of *L. rotata* exerting medicinal effects. Taking the intersection of compound targets and disease targets, 34 common targets were screened out. The relationship between them was predicted in String database, and PPI network visual analysis was performed on Cytoscape platform (Fig. 6B). It could be seen from the figure that matrix metalloproteinase 9 (*MMP9*), cyclooxygenase 2 (*PTGS2*) and estrogen receptor α (*ESR1*) were the key targets of the active ingredient of *L. rotata* acting on inflammation and immune response, indicating that these targets played an important pharmacological role in the treatment of RA.

Go analysis and KEGG analysis were carried out in David database, and the enrichment results were shown in Fig. 7. The results of GO analysis in biological processes included oxidation–reduction process, response to drug, negative regulation of apoptotic process, protein phosphorylation, collagen catabolic process, extracellular matrix disassembly and other biological processes (Fig. 7A). Enrichment in cellular component involved plasma membrane, integral component of membrane, nucleus, cytosol, extracellular space, et al (Fig. 7B). Enriched results in molecular function consisted of zinc ion binding, ATP binding, enzyme binding, protein homodimerization activity, protein kinase binding, identical protein binding and other molecular functions (Fig. 7C). In order to deeply understand the anti-rheumatoid arthritis mechanism of *L. rotata*, the KEGG pathway was enriched and analyzed. As a result, a total of 13 meaningful signal pathways were found, and enriched pathways with *P*-value < 0.05 were

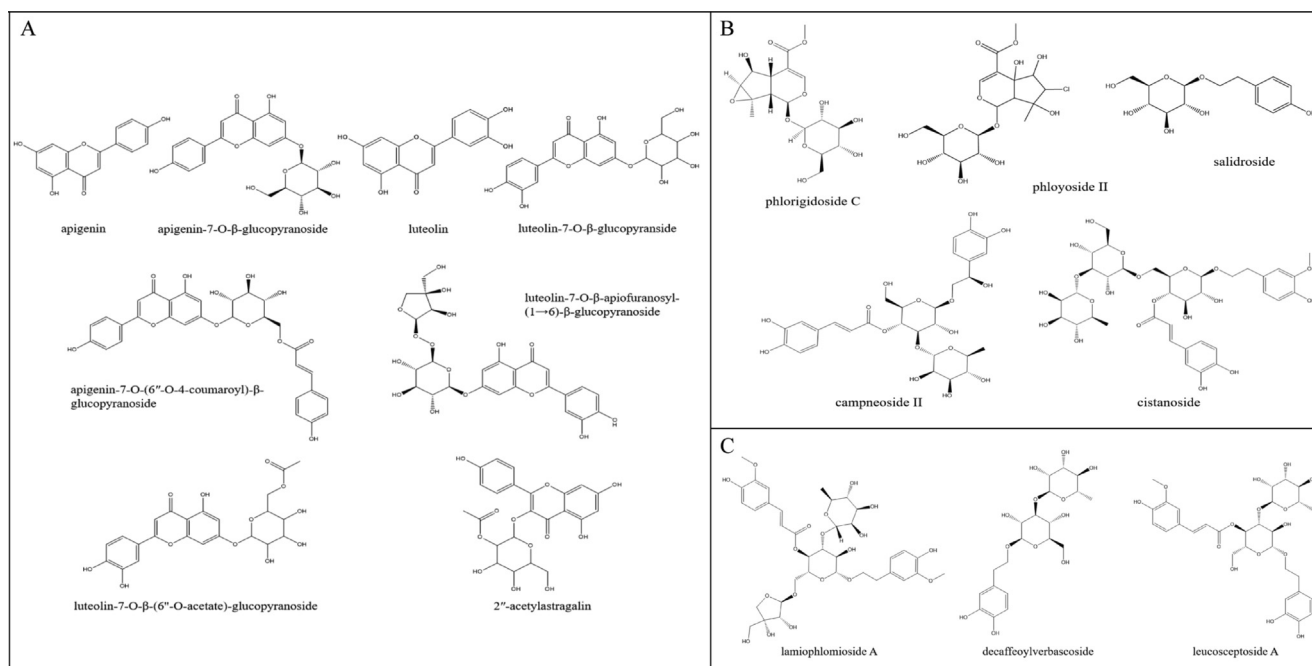


Fig. 4 Chemical structures of 16 differential metabolites. Characteristic components (A); higher difference components in aerial parts (B); higher difference components in roots (C).

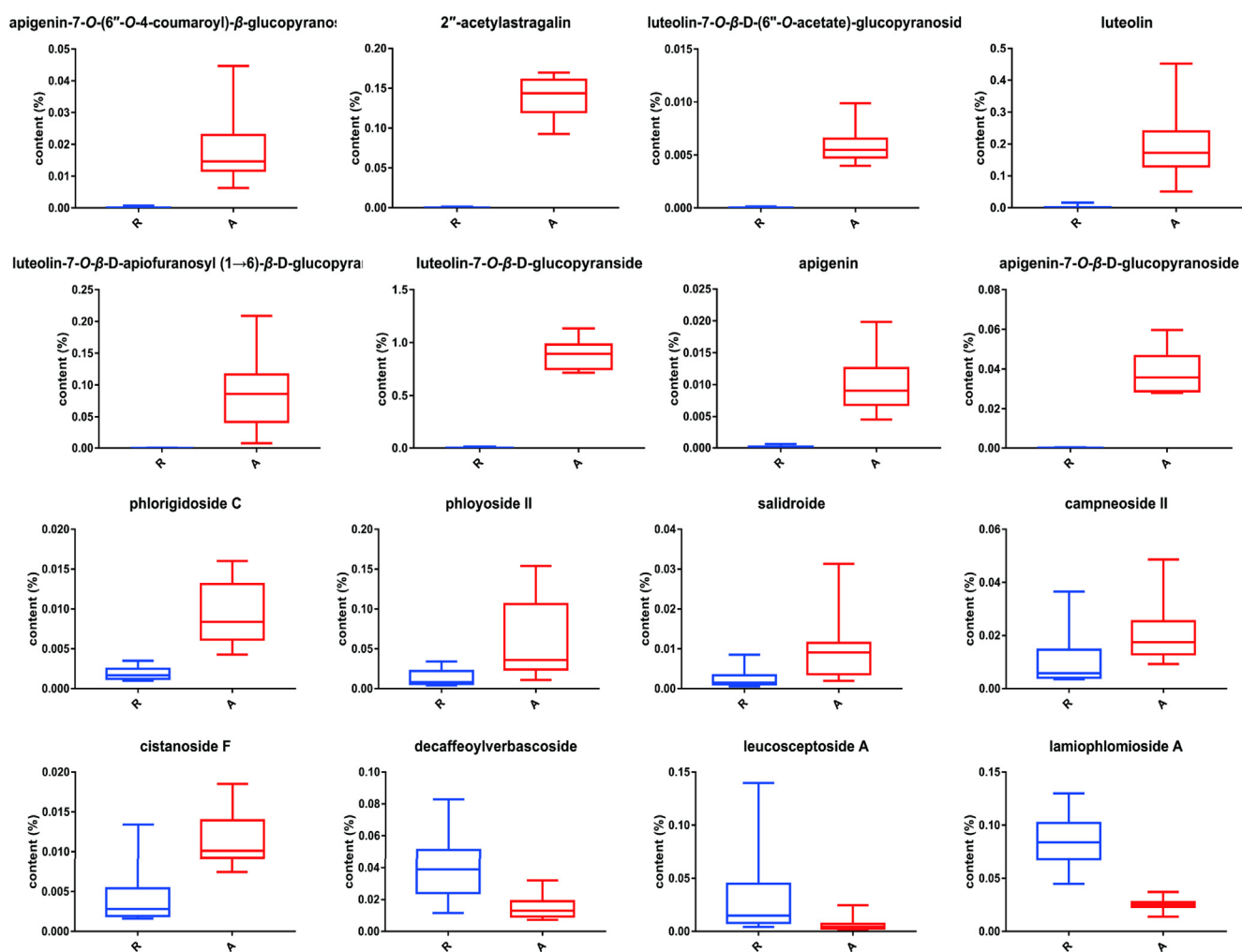


Fig. 5 Box plots of 16 different metabolites in aerial parts and roots.

collected in a bubble diagram (Fig. 7D), which included the steroid pathways and the cancer pathways accounted for the largest proportion, such as ovarian steroidogenesis, estrogen signaling pathway, steroid hormone biosynthesis, pathways in cancer, microRNAs in cancer and bladder cancer. Otherwise, there were also serotonergic synapse, ABC transporters, bile secretion and prolactin signaling pathway. Furthermore, the core analysis of the predicted pathway showed that RA was found in immune diseases (Fig. 7E).

In order to further reveal the relationship between active ingredients of *L. rotata* and RA effects, a component-target-pathway network was constructed. As shown in Fig. 6C, the chemical components associated with inflammation and immune pathways were flavonoids except caffeic acid, including 3 characteristic components screened from aerial parts and roots, namely apigenin, luteolin and 2''-acetylstragalalin. To some extent, it showed the superiority of the characteristic components (i.e., flavonoids) in aerial parts with the treatment of rheumatoid arthritis.

4. Discussion

Metabolomics originated from life science research, and later developed rapidly and penetrated completely into many

fields. At present, one of the branches is to apply the mass spectrometry results of chemical components and the research methods of metabolomics to the quality control of TCM (Yang et al., 2017). Through metabolomics analysis in different parts of the same Chinese medicinal materials, the different metabolites and potential markers between different parts are found to realize the purpose of recognition for different parts and quality control of TCM. A total of 16 different metabolites were identified in this study, and flavonoids were mainly focused in aerial parts, which could be used as a theoretical basis to distinguish aerial parts from roots. We speculate that the aerial part of *L. rotata* is a place where the density and strength of light are relatively concentrated, so that light may have a stress effect on flavonoids in plants. Some scholars pointed out that light probably worked by regulating the expression of related enzymes in flavonoid biosynthesis pathway (Pan et al., 2016), such as phenylalanine ammonia lyase (PAL) and chalcone synthase (CHS). As shown in Fig. 8, the basic skeleton of flavonoids was the biosynthetic product of three malonyl-CoA and one coumarinyl-CoA. Among them, coumarinyl-CoA was synthesized under the action of PAL using phenylalanine as a precursor, so PAL was the key enzyme and rate-limiting enzyme in the shikimate acid pathway. Malonyl-CoA and coumarinyl-CoA produced

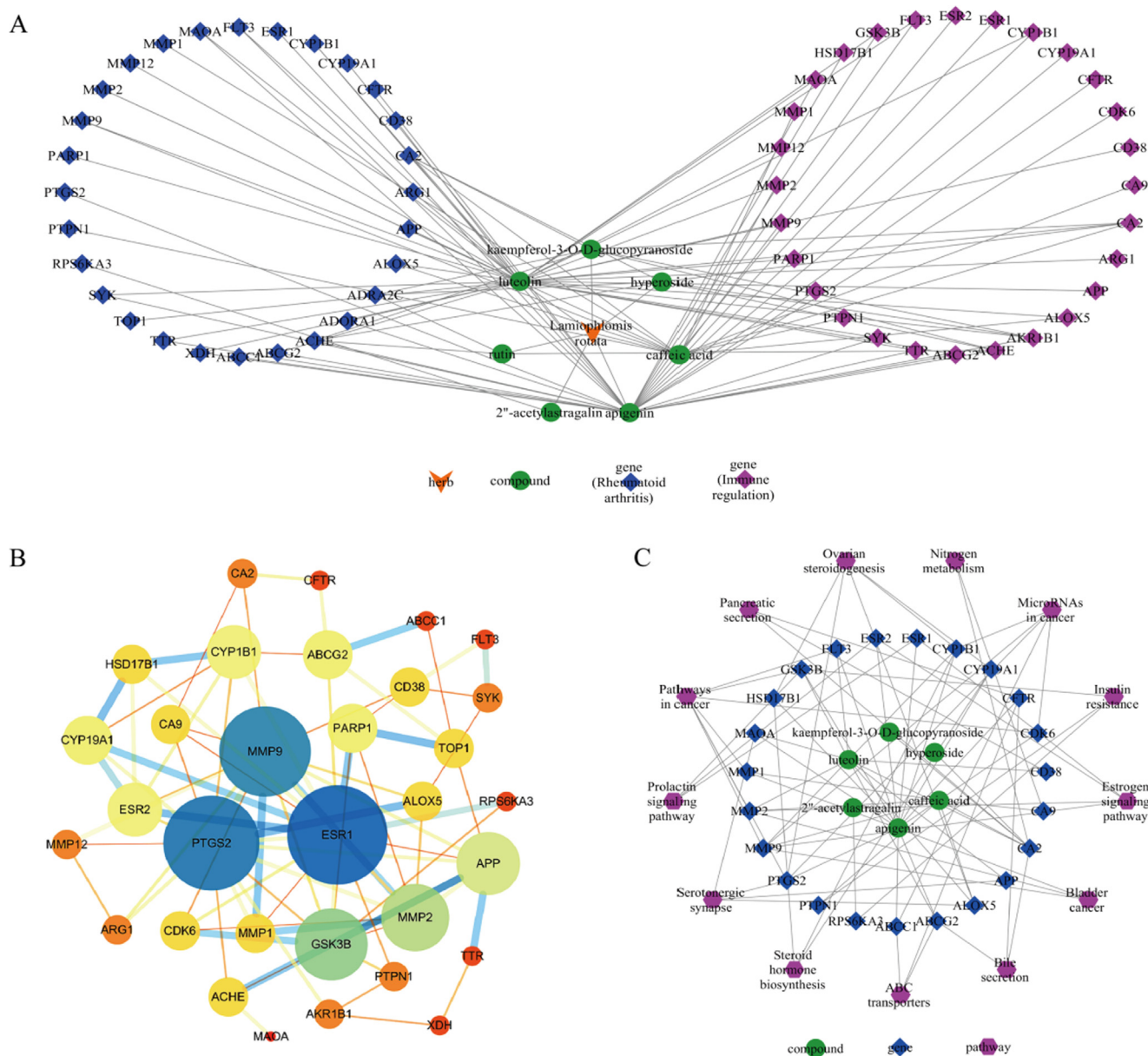


Fig. 6 *Lamiophlomis rotata* active ingredient - predicted target interaction network (A); protein-protein interaction network (B); *Lamiophlomis rotata* active ingredient - target - pathway network (C).

dihydroflavonoids under the action of CHS, and then other flavonoids were generated under the action of various enzymes. Therefore, CHS was the key enzyme connecting the two parts in the biosynthesis of flavonoids. Besides, as the quality parameters of Chinese Pharmacopoeia, shanzhiside methyl ester and 8-*O*-acetyl shanzhiside methyl ester are also characteristic components and active components of *L. rotata*. No significant difference was found between aerial parts and roots of the two components (this result was consistent with the previous results (Zhang et al., 2018).), which reflected the feasibility of aerial parts instead of whole herbs from the side.

Nowadays, mass spectrometry is the most frequently applied analytical detector in metabolomics, with the majority of separation platforms being UPLC based. Among them, the

hybrid Orbitrap mass spectrometer can provide higher mass resolution and higher mass accuracy. In this study, the Q-Exactive hybrid Q-Orbitrap mass spectrometer was used for full scan and MS/MS data collection to realize the detection of multiple secondary metabolites, which provided a basis for clarifying the main components and technical support for the rapid identification of *L. rotata* (Ossipov et al., 2020). A total of 48 components were identified in this study, mainly including 11 flavonoids, 17 iridoids, 14 phenylethanol glycosides and 6 other components. However, it was difficult to fully convincing the identification of each components by relying solely on mass spectrometry data. Therefore, it is necessary to use relevant separation methods to purify the identified components, and further confirm the chemical structure of

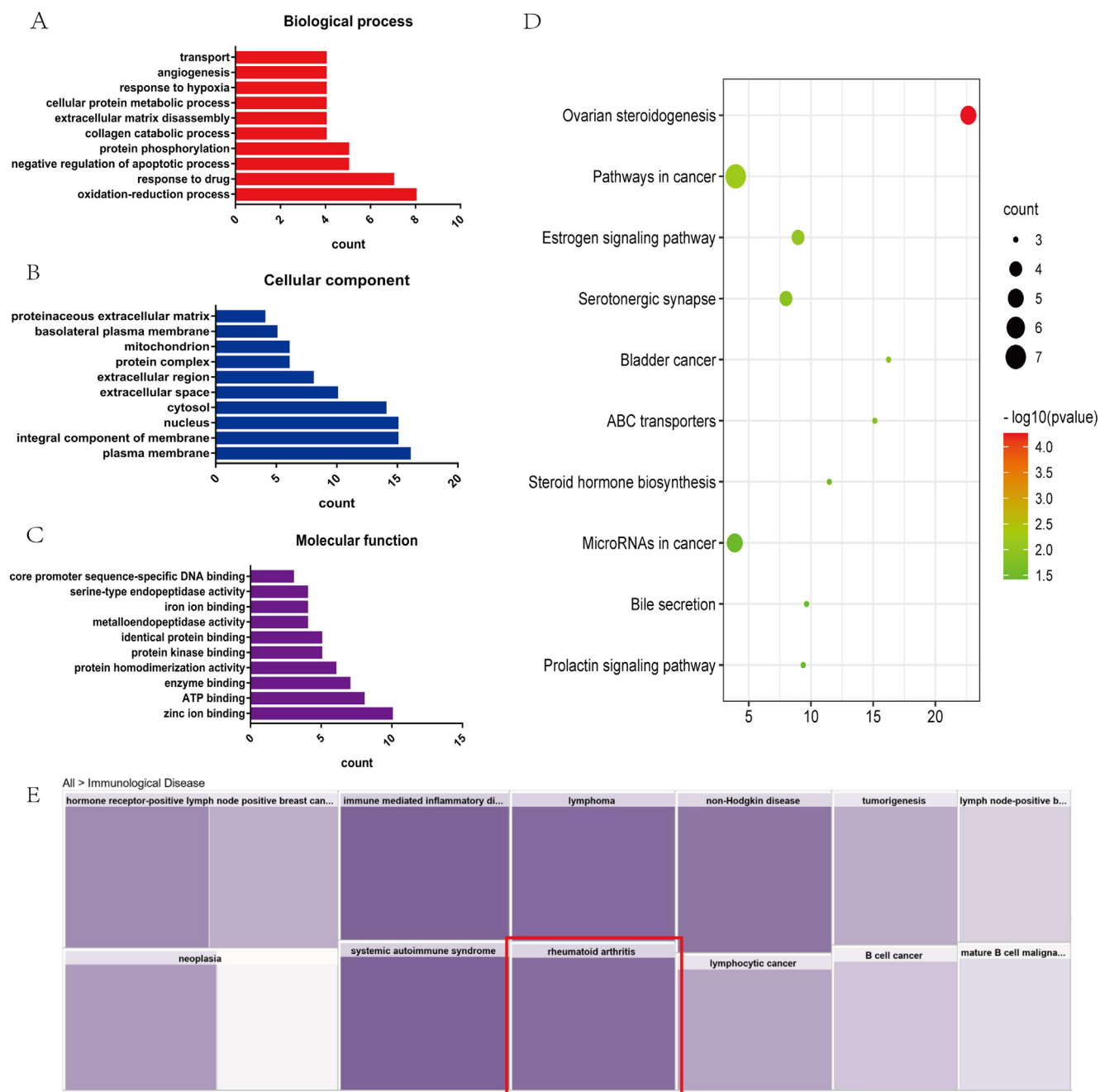


Fig. 7 GO enrichment analysis and KEGG enrichment signal pathways. The result of GO analysis in biological processes (A); Enrichment in cellular component (B); Enriched result in molecular function (C); enrichment analysis of KEGG pathway (D); core analysis of predicted pathway (E).

the isolated compounds by nuclear magnetic resonance and other technologies, so as to achieve the accurate identification of the chemical components of *L. rotata*.

As a modern means of activity prediction, network pharmacology is mainly used in many fields, such as pathogenesis exploration, drug development, drug target identification and so on (Kibble et al., 2015). In this study, the component targets were predicted based on the results of mass spectrometry, and then intersected with inflammatory and immune targets, which could reflect the anti-rheumatoid arthritis effect of *L. rotata* from different aspects. Among the different metabolites screened out, the component differences between aerial parts

and roots were mainly concentrated in flavonoids. Among the predicted active ingredients, the major active ingredients were also flavonoids. To a certain extent, the information reflected that the aerial parts might be more dominant in pharmacological efficacy, and provided a more powerful explanation for the aerial parts to replace the whole herbs. Of course, it was only the preliminary work of activity research, but which could play a leading role. In the later stage, it is necessary to conduct in-depth investigations in various aspects on different models.

As a traditional Tibetan medicine, *L. rotata* has a variety of pharmacological effects and has been clinically applied to treat

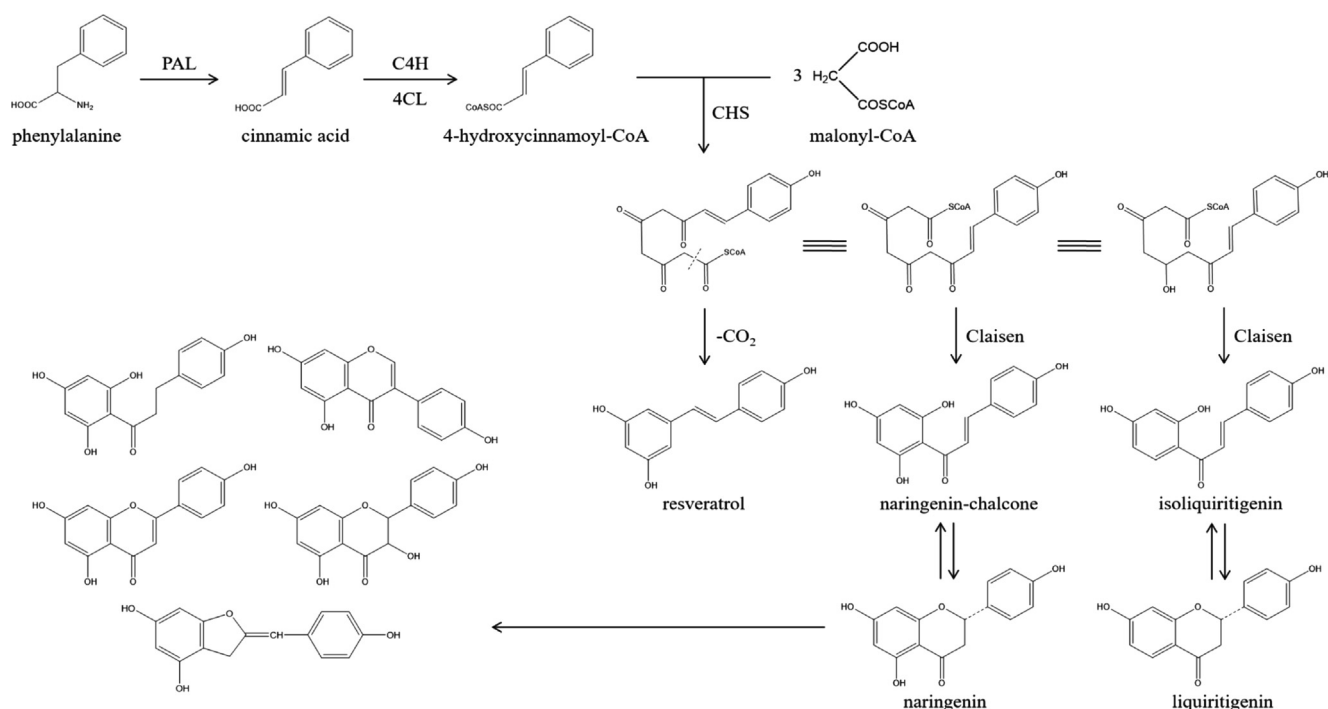


Fig. 8 Flavonoid biosynthesis pathway.

RA (Pan et al., 2015a). Unfortunately, environmental problems and growth disadvantages gradually emerged with the extensive development and application of *L. rotata*. Currently, the aerial parts have been promoted, and there have been literatures comparing the primary metabolites and iridoid glycosides in the aerial and underground parts (Pan et al., 2015b; Zhang et al., 2018). Therefore, this article was based on these study with all secondary metabolites in order to provide a theoretical basis of the chemical composition and pharmacological activity for the popularization of aerial parts in the future. This study mainly compared the differences of chemical components and pharmacological effects between aerial parts and roots by adopting the research method of interdisciplinary integration. First of all, the chemical composition network of different parts was constructed, then the analytical logic of network pharmacology was integrated, and finally the differences in composition and activity between aerial parts and roots were determined. This result means that flavonoids may be the focus of attention for comparison of different parts in the future.

In this study, 48 secondary metabolites were identified in the aerial parts and roots of *L. rotata*, which laid a foundation for the whole component analysis of this medicinal materials. Subsequently, 16 different metabolites were screened and quantified in aerial parts and roots, and 6 active components were predicted by network pharmacology. The results revealed that certain flavonoids as potential markers could make a distinction between aerial part and root of *L. rotata*, and the distribution of active components provided a theoretical basis for aerial parts to replace whole herbs, which contributed to the rational application of medicinal materials and promoted the development of ecology and resources in some way.

Author Contributions

Tong Li and Miaomiao Jiang conceived and designed the study. Tong Li, Ruijiao Du, Chengjuan Liu and Shengjie Huang performed the experiments. Tong Li and Li Jia were in charge of data curation. Tong Li wrote the original draft. Miaomiao Jiang, Heshui Yu, Lifeng Han, Xiaopeng Chen and Yuefei Wang reviewed and edited the manuscript. All authors read and approved the manuscript.

Declaration of Competing Interest

The authors declare that they have no known competing financial interests or personal relationships that could have appeared to influence the work reported in this paper.

Acknowledgements

This study was supported by the Natural Science Foundation of Tianjin City (No. 18JCZDJC97700), the Tianjin Science and Technology Program (Nos. 20ZYJJC00120 and 21ZYJJC00080), and the National Natural Science Foundation of China (No. 81573547).

Appendix A. Supplementary data

Supplementary data to this article can be found online at <https://doi.org/10.1016/j.arabjc.2022.103740>.

References

Aldini, G., Regazzoni, L., Pedretti, A., Carini, M., Cho, S.M., Park, K.M., et al. 2011. An integrated high resolution mass spectrometric and informatics approach for the rapid identification of phenolics

- in plant extract. *J Chromatogr A*. 1218, 2856–2864. <https://doi.org/10.1016/j.chroma.2011.02.065>.
- Amessis-Ouchemoukh, N., Abu-Reidah, I.M., Quirantes-Pin , R., Rodr guez-P rez, C., Madani, K., Fern ndez-Guti rrez, A., et al., 2014. Tentative characterisation of iridoids, phenylethanoid glycosides and flavonoid derivatives from *Globularia alypum* L. (Globulariaceae) leaves by LC-ESI-QTOF-MS. *Phytochem Anal.* 25, 389–398. <https://doi.org/10.1002/pca.2506>.
- Chinese pharmacopoeia., 2005. China Pharmacopoeia Committee. Pharmacopoeia of the People's Republic of China, Beijing.
- Chinese pharmacopoeia., 2010. China Pharmacopoeia Committee. Pharmacopoeia of the People's Republic of China, Beijing.
- Cui, Z.H., Qin, S.S., Zang, E.H., Li, C., Gao, L., Li, Q.C., et al., 2020. Traditional uses, phytochemistry, pharmacology and toxicology of *Lamiophlomis rotata* (Benth.) Kudo: a review. *RSC Adv.* 10, 11463. <https://doi.org/10.1039/d0ra01050b>.
- Dictionary of Chinese Materia Medica, 1977. Jiangsu New Medical College. Shanghai People's Publishing House, Shanghai.
- Dong, S.Q., Gao, R.B., Yang, Y., Guo, M., Ni, J.M., Zhao, L., 2014. Simultaneous determination of phenylethanoid glycosides and aglycones by capillary zone electrophoresis with running buffer modifier. *Anal Biochem.* 449, 158–163. <https://doi.org/10.1016/j.ab.2013.11.014>.
- Es-Safi, N.E., Kerhoas, L., Ducrot, P.H., 2007. Fragmentation study of iridoid glucosides through positive and negative electrospray ionization, collision-induced dissociation and tandem mass spectrometry. *Rapid Commun Mass Spectrom.* 21, 1165–1175. <https://doi.org/10.1002/rcm.2930>.
- Fan, P.C., Ma, H.P., Hao, Y., He, X.R., Sun, A.J., Jiang, W., et al., 2016. A new anti-fibrinolytic hemostatic compound 8-*O*-acetyl shanzhiside methylester extracted from *Lamiophlomis rotata*. *J Ethnopharmacol.* 187, 232–238. <https://doi.org/10.1016/j.jep.2016.04.016>.
- Fan, P.C., Ma, H.P., Jing, L.L., Li, M.X., He, X.R., Jia, Z.P., 2012. Simultaneous isolation and preparation of four iridoid glycosides from *Lamiophlomis rotata* by preparative RP-HPLC. *Chinese Traditional and Herbal Drugs.* 43, 699–701.
- Frid n, M.E., S jberg, P.J., 2014. Strategies for differentiation of isobaric flavonoids using liquid chromatography coupled to electrospray ionization mass spectrometry. *J Mass Spectrom.* 49, 646–663. <https://doi.org/10.1002/jms.3386>.
- Guo, N., Ding, W.M., Wang, Y., Hu, Z.W., Wang, Z.M., Wang, Y., 2014. An LC-MS/MS method for the determination of salidroside and its metabolite *p*-tyrosol in rat liver tissues. *Pharm Biol.* 52, 637–645. <https://doi.org/10.3109/13880209.2013.863946>.
- Han, J.S., Lee, S., Kim, H.Y., Lee, C.H., 2015. MS-Based Metabolite Profiling of Aboveground and Root Components of *Zingiber mioga* and *Officinale*. *Molecules.* 20, 16170–16185. <https://doi.org/10.3390/molecules200916170>.
- Han, L.F., Boakye-Yiadom, M., Liu, E.W., Zhang, Y., Li, W., Song, X.B., et al., 2012. Structural characterisation and identification of phenylethanoid glycosides from *Cistanches deserticola* Y.C. Ma by UHPLC/ESI-QTOF-MS/MS. *Phytochem Anal.* 23, 668–676. <https://doi.org/10.1002/pca.2371>.
- Ji, L.J., Feng, L.J., Li, S.P., Zhao, M.C., 2007. Analysis of luteolin and total flavonoids in different parts of Tibetan medicine *Lamiophlomis rotata*. *Chinese Journal of Analysis Laboratory.* 26, 101–103.
- Jia, Z.P., Li, M.X., Zhang, R.X., Shen, T., Fei, G.S., 2005. Experimental Study on the Effective Hemostatic Components of Herba *Lamiophlomis Rotata*. *Pharm J Chin PLA.* 21, 272–274.
- Jiang, W.L., Fu, F.H., Xu, B.M., Tian, J.W., Zhu, H.B., Hou, J., 2010a. Cardioprotection with forsythoside B in rat myocardial ischemia-reperfusion injury: relation to inflammation response. *Phytomedicine.* 17, 635–639. <https://doi.org/10.1016/j.phymed.2009.10.017>.
- Jiang, W.L., Fu, F.H., Zheng, S.H., Zhang, D.L., Zhu, H.B., Hou, J., 2010b. 8-*O*-acetyl shanzhiside methylester attenuates apoptosis and ameliorates mitochondrial energy metabolism in rat cortical neurons exposed to oxygen-glucose deprivation. *Eur J Pharmacol.* 629, 20–24. <https://doi.org/10.1016/j.ejphar.2009.11.065>.
- Jiang, W.L., Zhang, S.P., Fu, F.H., Zhu, H.B., Hou, J., 2010c. Inhibition of nuclear factor- κ B by 6-*O*-acetyl shanzhiside methyl ester protects brain against injury in a rat model of ischemia and reperfusion. *J Neuroinflammation.* 7, 55. <https://doi.org/10.1186/1742-2094-7-55>.
- Kang, Z.C., Jiang, W.L., Xu, Y., Zhu, H.B., Hou, J., 2012. Cardioprotection with 8-*O*-acetyl shanzhiside methylester on experimental myocardial ischemia injury. *Eur J Pharm Sci.* 47, 124–130. <https://doi.org/10.1016/j.ejps.2012.05.011>.
- Kibble, M., Saarinen, N., Tang, J., Wennerberg, K., M kel , S., Aittokallio, T., 2015. Network pharmacology applications to map the unexplored target space and therapeutic potential of natural products. *Nat Prod Rep.* 32, 1249–1266. <https://doi.org/10.1039/c5np00005j>.
- Kim, H.Y., Lee, M.Y., Park, H.M., Park, Y.K., Shon, J.C., Liu, K.H., et al., 2015. Urine and serum metabolite profiling of rats fed a high-fat diet and the anti-obesity effects of caffeine consumption. *Molecules.* 20, 3107–3128. <https://doi.org/10.3390/molecules20023107>.
- Kim, Y.M., Lee, J., Park, S.H., Lee, C., Lee, J.W., Lee, D., Kim, N., et al., 2012. LC-MS-based chemotaxonomic classification of wild-type *Lepedeza* sp. and its correlation with genotype. *Plant Cell Rep.* 31, 2085–2097. <https://doi.org/10.1007/s00299-012-1319-8>.
- Ku, K.M., Choi, J.N., Kim, J., Kim, J.K., Yoo, L.G., Lee, S.J., et al., 2009. Metabolomics analysis reveals the compositional differences of shade grown tea (*Camellia sinensis* L.). *J Agric Food Chem.* 58, 418–426. <https://doi.org/10.1021/jf902929h>.
- La, M.P., Zhang, F., Gao, S.H., Liu, X.W., Wu, Z.J., Sun, L.N., et al., 2015. Constituent analysis and quality control of *Lamiophlomis rotata* by LC-TOF/MS and HPLC-UV. *J Pharm Biomed Anal.* 102, 366–376. <https://doi.org/10.1016/j.jpba.2014.09.038>.
- Lee, S., Seo, M.H., Oh, D.K., Lee, C.H., 2014. Targeted metabolomics for *Aspergillus oryzae*-mediated biotransformation of soybean isoflavones, showing variations in primary metabolites. *Biosci Biotechnol Biochem.* 78, 167–174. <https://doi.org/10.1080/09168451.2014.877827>.
- Li, C.M., Zhang, X.L., Xue, X.Y., Zhang, F.F., Xu, Q., Liang, X.M., 2008. Structural characterization of iridoid glucosides by ultra-performance liquid chromatography/electrospray ionization quadrupole time-of-flight tandem mass spectrometry. *Rapid Commun Mass Spectrom.* 22, 1941–1954. <https://doi.org/10.1002/rcm.3579>.
- Li, M.X., Zhang, R.X., Jia, Z.P., Sheng, J., Qiu, J.G., Wang, J., 2009. Isolation and identification of hemostatic ingredients from *Lamiophlomis rotata* (Benth.) Kudo. *Phytother Res.* 23, 816–822. <https://doi.org/10.1002/ptr.2669>.
- Liu, H.F., Li, X., Deng, B., Song, X., Li, H., 2006. Study on the chemical constituents of the essential oil from *Lamiophlomis rotata*. *Chin J Pharm Anal.* 26, 1794–1796.
- Luo, M.N., Lu, H.W., Ma, H.Q., Zhao, L., Liu, X., Jiang, S.X., 2007. Separation and determination of flavonoids in *Lamiophlomis rotata* by capillary electrophoresis using borate as electrolyte. *J. Pharm. Biomed. Anal.* 44, 881–886. <https://doi.org/10.1016/j.jpba.2007.04.010>.
- Mendes, P., 2006. Metabolomics and the challenges ahead. *Brief Bioinform.* 7, 127. <https://doi.org/10.1093/bib/bbl010>.
- Ossipov, V., Koivuniemi, A., Mizina, P., Salminen, J.P., 2020. UPLC-PDA-Q Exactive Orbitrap-MS profiling of the lipophilic compounds product isolated from *Eucalyptus viminalis* plants. *Heliyon.* 6, <https://doi.org/10.1016/j.heliyon.2020.e05768> e05768.
- Pan, J.Q., Tong, X.R., Guo, B.L., 2016. Progress of effects of light on plant flavonoids. *China Journal of Chinese Materia Medica.* 41, 3897–3903.
- Pan, Z., Fan, G., Yang, R.P., Luo, W.Z., Zhou, X.D., Zhang, Y., 2015a. Discriminating *Lamiophlomis rotata* According to Geographical Origin by (1)H-NMR Spectroscopy and Multivariate

- Analysis. *Phytochem Anal.* 26, 247–252. <https://doi.org/10.1002/pca.2557>.
- Pan, Z., Mao, Q., Jiang, S., Fan, G., Zhang, Y., 2015b. *Metabonomics and pattern recognition study on the different parts of Lamiophlomis rotata* (Benth.) Kudo. *Chinese Traditional Patent Medicine.* 37, 567–570.
- Qi, L.W., Chen, C.Y., Li, P., 2009. Structural characterization and identification of iridoid glycosides, saponins, phenolic acids and flavonoids in Flos *Lonicerae Japonicae* by a fast liquid chromatography method with diode-array detection and time-of-flight mass spectrometry. *Rapid Commun Mass Spectrom.* 23, 3227–3242. <https://doi.org/10.1002/rcm.4245>.
- Sanz, M., de Simón, B.F., Cadahia, E., Esteruelas, E., Muñoz, A.M., Hernández, T., et al, 2012. LC-DAD/ESI-MS/MS study of phenolic compounds in ash (*Fraxinus excelsior* L. and *F. americana* L.) heartwood. Effect of toasting intensity at cooperage. *J Mass Spectrom.* 47, 905–918. <https://doi.org/10.1002/jms.3040>.
- Sun, H.Y., Liu, M.X., Lin, Z.T., Jiang, H.X., Niu, Y.Y., Wang, H., et al, 2015. Comprehensive identification of 125 multifarious constituents in Shuang-huang-lian powder injection by HPLC-DAD-ESI-IT-TOF-MS. *J Pharm Biomed Anal.* 115, 86–106. <https://doi.org/10.1016/j.jpba.2015.06.013>.
- Tao, R., Li, M.X., Zhang, Q.L., Qiu, J.G., Zhang, J.H., Jia, Z.P., 2014. Isolation and Identification of Nine Iridoid Glycosides from *Lamiophlomis rotata* by HPLC Combining PDA and MS. *Journal of Chinese Medicinal Materials.* 37, 439–442. <https://doi.org/10.13863/j.issn1001-4454.2014.03.029>.
- Van der Hoof, J.J., Vervoort, J., Bino, R.J., Beekwilder, J., de Vos, R. C., 2011. Polyphenol identification based on systematic and robust high-resolution accurate mass spectrometry fragmentation. *Anal Chem.* 83, 409–416. <https://doi.org/10.1021/ac102546x>.
- Wang, J., Gao, Y.L., Chen, Y.L., Chen, Y.W., Zhang, Y., Xiang, L., et al, 2018. *Lamiophlomis rotata* Identification via ITS2 Barcode and Quality Evaluation by UPLC-QTOF-MS Couple with Multivariate Analyses. *Molecules.* 23, 3289. <https://doi.org/10.3390/molecules23123289>.
- Wang, Y.L., Cui, T., Li, Y.Z., Liao, M.L., Zhang, H.B., Hou, W.B., et al, 2019. Prediction of quality markers of traditional Chinese medicines based on network pharmacology. *Chin Herb Med.* 11, 349–356.
- Wu, L., Li, L., Wang, M., Shan, C., Cui, X., Wang, J., et al, 2016. Target and non-target identification of chemical components in *Lamiophlomis rotata* by liquid chromatography/quadrupole time-of-flight mass spectrometry using a three-step protocol. *Rapid Commun Mass Spectrom.* 30, 2145–2154. <https://doi.org/10.1002/rcm.7695>.
- Yang, W.Z., Zhang, Y.B., Wu, W.Y., Huang, L.Q., Guo, D.A., Liu, C.X., 2017. Approaches to establish Q-markers for the quality standards of traditional Chinese medicines. *Acta Pharm Sin B.* 7, 439–446. <https://doi.org/10.1016/j.apsb.2017.04.012>.
- Yue, H.L., Zhao, X.H., Mei, L.J., Shao, Y., 2013. Separation and purification of five phenylpropanoid glycosides from *Lamiophlomis rotata* (Benth.) Kudo by a macroporous resin column combined with high-speed counter-current chromatography. *J Sep Sci.* 36, 3123–3129. <https://doi.org/10.1002/jssc.201300268>.
- Zan, K., Guo, L.N., Ma, S.C., Zheng, J., 2018. Analysis of Thirty Chemical Constituents in Tibetan Medicine *Lamiophlomis rotata* by UPLC-ESI-TOF MS. *Chinese Pharmaceutical Affairs.* 32, 757–763. <https://doi.org/10.16153/j.1002-7777.2018.06.011>.
- Zeng, Y., Chen, X.X., Chen, Z.N., 2001. Advances in studies on traditional Tibetan herb *Lamiophlomis rotata*. *Chinese Traditional and Herbal Drugs.* 32, 88–90.
- Zhang, D., Gao, Y.L., Jiang, S., Chen, Y.W., Zhang, Y., Pan, Z., 2018. The similarity and variability of the iridoid glycoside profile and antioxidant capacity of aerial and underground parts of *Lamiophlomis rotata* according to UPLC-TOF-MS and multivariate analyses. *RSC Adv.* 8, 2459. <https://doi.org/10.1039/c7ra10143k>.
- Zhang, F., Wu, Z.J., Sun, L.N., Wang, J., Tao, X., Chen, W.S., 2012. Iridoid glucosides and a C₁₃-norisoprenoid from *Lamiophlomis rotata* and their effects on NF- κ B activation. *Bioorg Med Chem Lett.* 22, 4447–4452. <https://doi.org/10.1016/j.bmcl.2012.04.087>.
- Zhang, Q.L., Qiu, J.G., Li, M.X., Wei, L.L., He, X.R., Jia, Z.P., 2011. Hemostatic Effects of Externally Application of the Effective Components from Herba *Lamiophlomis Rotata*. *Herald of Medicine.* 30, 877–879.
- Zhang, Y.F., Chen, R.X., Yuan, M.H., Yang, Z.Z., Huang, T., Chen, S.X., et al, 2021. Study on Effects and Active Ingredients of Tibetan Medicine *Lamiophlomis rotata* against Rheumatoid Arthritis. *China Pharmacy.* 32, 578–583.
- Zhao, S.G., 2004. Pharmacology and clinical application of *Lamiophlomis rotata*. *Lishizhen Medicine and Materia Medica Research.* 15, 873.
- Zheng, Y.N., Yin, X.F., Huo, F.Q., Xiong, H., Mei, Z.N., 2015. Analgesic effects and possible mechanisms of iridoid glycosides from *Lamiophlomis rotata* (Benth.) Kudo in rats with spared nerve injury. *J Ethnopharmacol.* 173, 204–211. <https://doi.org/10.1016/j.jep.2015.06.045>.